Finite-size effect for the critical point of an anisotropic dimer model of domain walls

Somendra M. Bhattacharjee* and John F. Nagle
Department of Physics, Carnegie Mellon University, Pittsburgh, Pennsylvania 15213
(Received 24 September 1984)

The finite-size effect is studied in the Kasteleyn model of dimers on the brick lattice. This model is isomorphic to an anisotropic domain-wall model. Asymptotic analysis of the exact Pfaffian solution for the specific heat establishes that finite-size-scaling theory is valid near the critical point of this model. The finite-size-scaling function is a function of a scaled temperature variable τ and a shape factor $\kappa=N^2/M$, where $2N$ is the number of lattice points in the direction perpendicular to the preferred axis for the domain walls and $2M$ is the number of lattice points parallel to the preferred axis. The scaled temperature variable τ is given by $MN^2t/(M+N^2)$, where t is the reduced temperature. As a function of τ the scaling function $\mathcal{P}(\tau,\kappa)$ is a sequence of δ functions in the limit $\kappa=0$ and a smooth single-peaked function in the limit $\kappa=\infty$. In the latter case the specific heat per lattice site can be written as $M^{\alpha/\nu_M}\mathcal{P}(tM^{1/\nu_M},\infty)$, where α is the bulk specific-heat exponent with the known value of $\frac{1}{2}$ and ν_M is found to have the value of 1. In the case $\kappa=0$, the specific heat per lattice site can be written in an equivalent form by replacing M by N and ν_m by ν_N which takes the value $\nu_N=\frac{1}{2}$. According to finite-size-scaling theory ν_M and ν_N may be interpreted to be the critical exponents ν_y and ν_x, respectively, of the divergent length scales in the two principal directions. Our exact values of ν_m and ν_N are in agreement with the values of ν_y and ν_x predicted for general anisotropic domain-wall models.

I. INTRODUCTION

About twenty years ago Kasteleyn[1] introduced a dimer model on an anisotropic honeycomb lattice, which is aptly described as a brick lattice, as shown in Fig. 1. Each state of this model, which has been called the Kasteleyn model (or K model),[2] consists of a complete covering of the sites of the brick lattice by dimers, each of which covers two nearest-neighbor lattice sites and the connecting bond. Dimers on vertical bonds have zero energy and dimers on horizontal bonds have an energy ϵ. This difference in energy for dimers lying in different directions creates the spatial anisotropy that breaks the symmetry of the topologically equivalent honeycomb lattice. The total energy E_s of any state is just the sum of the energies of the individual dimers. Cooperativity is due to the excluded volume constraint that does not allow two dimers to occupy the same lattice site; there are no softer interactions between neighboring dimers in this model. As for any planar dimer model of this type, the partition function[3] $Z=\sum_{\text{states}}\exp(-\beta E_s)$ can be determined exactly, for finite or infinite lattices, by the Pfaffian technique.[4–6]

The exact solution of the K model in the thermodynamic limit of an infinite lattice size reveals an unusual phase transition.[1] The specific heat has a square-root divergence[3] ($\alpha=\frac{1}{2}$) at $T_c=\epsilon/(k_B\ln 2)$ as T is lowered toward T_c, but the specific heat is identically zero for all T smaller than T_c. This phase transition behavior contrasts strongly with the symmetrical logarithmic divergence of the traditional planar Ising models.[7,8] Some purely dimeric models that cannot be formulated as Ising models, such as the dimer model on the "4-8 lattice,"[9] also share the more traditional symmetric logarithmic specific-heat divergence. Other dimer models have been found that behave similarly to the K model.[10,11] It is useful to think of three universality classes of models that can be solved exactly by the Pfaffian method; the Ising class, the Kasteleyn class and a third class that is less interesting because it includes models, such as dimers on a rectangular lattice,[4,12] that have no phase transition. Although it is not proven that this classification scheme is complete nor is it perfectly clear what diagnostics, short

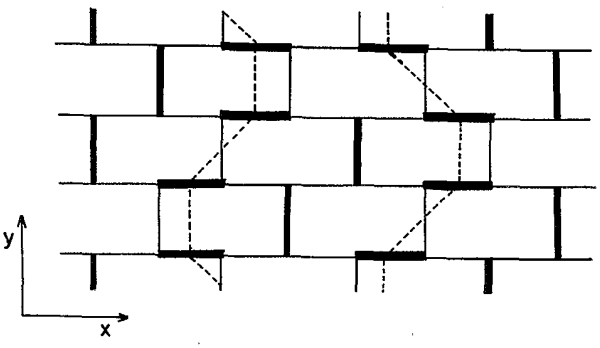

FIG. 1. One state of the K model on a finite brick lattice with periodic boundary conditions. There are $2N=8$ lattice points in the horizontal x direction and $2M=4$ lattice points in the vertical y direction. Each of the eight horizontal dimers (thick lines) costs energy ϵ [activity $x\equiv\exp(-\beta\epsilon)$ (Ref. 3)] while the four vertical dimers cost no energy (activity=1). The noncolliding domain walls (dashed lines) are obtained by connecting the centers of the horizontal dimers. Two horizontal dimers are connected if and only if they have a common adjacent vertical bond.

of a full exact solution, determine which class a given model will fall into, models in the Kasteleyn class seem to have a conservation (or forcing) property that requires the correlation functions to be long range with algebraic, rather than exponential, decay with distance.[13,14] This forcing property is very easy to see in the K model. If one starts in the ground state with all dimers on the vertical bonds and tries to shift one dimer onto a horizontal bond, then one must shift a vertical dimer onto a horizontal bond on each of the horizontal layers, from top to bottom, in the whole lattice. For example, in the state shown in Fig. 1 there are two horizontal dimers in the first row which requires that there be two horizontal dimers in each row. For infinite lattices this requires an infinite amount of energy. As a consequence, the excited states of the K model are separated by infinite energy gaps from the ground state and also from each other.

The aforementioned forcing property of models in the Kasteleyn class has sometimes been thought to be artificial, especially if one is thinking of fluids or magnetism. However, this property is very natural for two much different kinds of physical system. The first such system, which has been elaborated upon in the past,[15] is lipid bilayer biomembranes, for which the forcing property translates to the fact that the linear unbranched hydrocarbon chains can not end or begin arbitrarily. (The dimer model one needs[11] for this system is shown in Fig. 2. This model, to be called the generalized K model, is characterized by two parameters x and y and includes the K model as the $y=0$ case.) The second such system, which will be discussed more fully here, is a domain-wall model of the commensurate-incommensurate (CI) transition.[16] The isomorphism[17,18] of the K model to a domain-wall model is shown in Fig. 1. The anisotropy of the K model translates to the domain walls lying along the **y** axis and the forcing property of the K model translates to the domain walls not being allowed to begin, end, or annihilate each other as they proceed along the **y** axis. This isomorphism and the exact solution of the K model have provided rigorous tests of some of the theories[18] of the $p\times 1$ CI transitions. It might also be mentioned that a dimer model where the walls can meet and annihilate in pairs has recently been introduced.[19] Its exact solution allows the testing of theories of CI-Ising crossover.[20]

A phenomenological theory of the critical point exponents for $p\times 1$ CI transitions based on the domain-wall picture has recently been developed.[21,20] Two length scales have been proposed; one, ξ_y, pertains to the direction parallel to the domain walls; the other, ξ_x, pertains to the transverse direction. According to this theory, these length scales ξ_x and ξ_y diverge near the critical point with two different critical exponents[3] $\nu_x=\frac{1}{2}$ and $\nu_y=1$. These values of ν_x and ν_y satisfy the hyperscaling relation generalized to anisotropic systems,[21] namely $\nu_x+\nu_y=2-\alpha$ and α equals $\frac{1}{2}$ as in the K model. One of the results of this paper will be to demonstrate that the phenomenological theory is consistent with extensive additional exact results for the K model on finite lattices. This demonstration involves use of the concepts of finite-size-scaling theory[22] and our exact calculations demonstrate that this theory, when suitably generalized to anisotropic models, is valid for the K model.

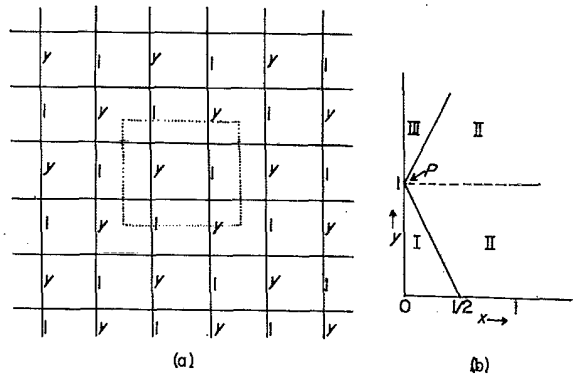

FIG. 2. (a) The generalized K model on a square lattice of shape $N\times M$ with $2M=6$ lattice points in the vertical direction and $2N=6$ lattice points in the horizontal direction. The horizontal bonds have activity x while the vertical bonds have activities 1 and y alternately as shown. The K model corresponds to $y=0$. This generalized model belongs to the Kasteleyn class for $y\neq 1$ and belongs to the third class for $y=1$, when it is just the rectangular lattice model. A unit cell for the Pfaffian solution is shown by the dotted lines. (See also Ref. 11.) This unit cell is chosen because of the periodic boundary conditions in the two principal lattice directions. (b) The phase diagram of the generalized K model in the (x,y) activity plane. In phase I, the system is frozen in the ground state where the dimers are on the bonds of activity 1 ($y<1$). Phase III is also a frozen state where the dimers are on the edges of activity y ($y>1$). Phase II is the disordered phase. P is a multicritical point. The dashed line corresponds to the rectangular lattice model and there is no nonanalyticity as one crosses this line by changing y, except at P.

Since the finite-size-scaling theory plays a crucial role in this paper, we give a brief review of it here. Figure 3 shows the specific heat $c_{\infty\times\infty}(T)$ of the K model on a lattice infinite in both directions ($\infty\times\infty$ lattice). Also shown there are the specific heats $c_{\infty\times M}(T)$ for different values of M when the lattice is finite in the vertical direction with $2M$ lattice points (i.e., with M unit cells) and infinite in the horizontal direction ($\infty\times M$ lattice). Now, as the limit $M\to\infty$ is taken at a fixed temperature $T(\neq T_c)$, $c_{\infty\times M}(T)$ must approach $c_{\infty\times\infty}(T)$ so that the error $R_M(T)=c_{\infty\times\infty}(T)-c_{\infty\times M}(T)$ approaches zero. However, right at $T=T_c$ the specific heat for any finite value of M remains finite so that the error term $R_M(T_c)$ has to be as significant as the bulk term. This means that breaking up $c_{\infty\times M}(T)$ as a bulk term plus some correction term is not possible at or close to T_c. Finite-size-scaling theory[22] is designed to provide an asymptotic form that works in this critical region. Various limiting procedures are shown schematically in Fig. 4.

The central concept of finite-size-scaling theory is that, if a critical point is characterized by a divergent length scale ξ with an exponent[3] ν, then finite-size effects will become substantial only when the size of the system is comparable to this length scale ξ. Close to the critical temperature it is supposed that any thermodynamic function, such as the specific heat, can be written in a scaling form

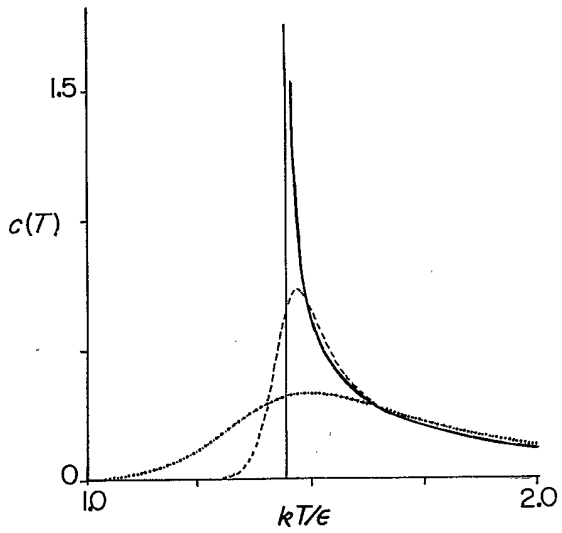

FIG. 3. The finite-size effect for the specific heat per lattice site, c, of the K model (Fig. 1) as a function of temperature T for a few different sizes. For a doubly infinite system the (bulk) specific heat $c_{\infty\times\infty}(T)$ is shown by the solid line. The vertical line indicates the bulk transition temperature T_c. For finite M and infinite N the specific heats $c_{\infty\times M}(T)$ are shown by a dotted line for $M=10$ and by a dashed line for $M=20$.

$$c(t)\approx M^{\omega_M}\mathscr{P}(tM^{1/\nu_M})\,, \tag{1.1}$$

where ω_M and ν_M are the two exponents characterizing the finite-size effect, M is a length characteristic of the finiteness of the system and t is the reduced temperature, $(T-T_c)/T_c$. The argument of the function $\mathscr{P}$ in Eq. (1.1), namely tM^{1/ν_M}, must be related to the ratio of M to ξ since ξ is assumed to be the only intrinsic length scale available with which to compare the finite size M. (M and N will be referred to as lengths, although formally

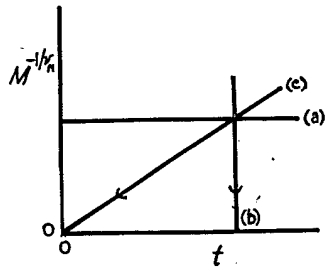

FIG. 4. Schematic diagram showing various limiting procedures for simple finite-size scaling theory for isotropic systems. The vertical axis is the inverse of the size of the system raised to the $1/\nu_M$ power and the horizontal axis is the reduced temperature (Ref. 3) t. The origin represents the bulk critical point. The trajectory indicated by the horizontal line (a) corresponds to scanning the temperature of a fixed finite-size lattice, with specific heats as shown in Fig. 3. The trajectory indicated by the vertical line (b) corresponds to taking the thermodynamic limit at a fixed temperature. The trajectory indicated by (c) maintains constant $\tau_M=tM^{1/\nu_M}$. Finite-size scaling theory makes predictions for such a trajectory (c) as the origin is approached.

one should multiply them by the lattice spacing which, however, can be set equal to 1.) Therefore, $tM^{1/\nu_M}\sim(M/\xi)^{1/\nu_M}$ which implies that $\nu_M=\nu$ since ν is defined through $\xi\sim t^{-\nu}$. Moreover, one requires that the form in Eq. (1.1) should give the bulk behavior $c(t)\approx C_\pm t^{-\alpha}$ as $M\to\infty$. Therefore, to obtain the proper t dependence one must have $\mathscr{P}(z)\approx C_\pm|z|^{-\alpha}$ as $z\to\pm\infty$. Eliminating the M dependence requires $\omega_M=\alpha/\nu_M$. Together with $\nu_M=\nu$ this shows that the finite-size exponents are related to the bulk exponents. The scaling form is, therefore, given by

$$c(t)\approx M^{\alpha/\nu}\mathscr{P}(tM^{1/\nu})\,. \tag{1.2}$$

Note that the identification of ν_M as ν, though highly plausible, is really a hypothesis of the scaling theory because one has to compare M with the bulk length scale ξ which, strictly speaking, does not exist in the finite system. However, the dependence of ω_M on α is a requirement, and not a hypothesis, once Eq. (1.1) is accepted. If the finite system does not show any critical behavior, then one can identify[22] the position of the maximum specific heat as a pseudocritical temperature T_m: as $M\to\infty$, T_m must approach T_c. Assuming a power-law dependence[22]

$$t_m\equiv\frac{T_m-T_c}{T_c}\approx\frac{b}{M^\lambda} \tag{1.3}$$

in the limit $M\to\infty$, one can again use the argument that ξ is the only length scale to conclude that the shift exponent λ must be equal to $1/\nu$. It may also be noted that the divergence of the total specific heat right at the critical temperature $t=0$ goes as $M^{\alpha/\nu}$.

In this paper we perform exact calculations to study the finite-size effect of the critical behavior of the K model with periodic boundary conditions. We use the usual methods of asymptotic expansions[23] to obtain the finite-size-scaling behavior of the specific heat as the thermodynamic limit is taken. Such methods have been used by Ferdinand[24] to calculate the expansion of the free energy of the rectangular lattice dimer model at a fixed temperature away from the multicritical point P of Fig. 2 (i.e., along the dotted line). Later Ferdinand and Fisher[25] used these methods to obtain the finite-size-scaling behavior for the square lattice Ising model. For the rectangular lattice dimer model the approach to the thermodynamic limit at a fixed temperature is algebraic and not exponential as it is in the Ising model when T is not equal to T_c. One of us has also performed extensive calculations on the K model and the generalized K model at a fixed temperature.[26] Like the rectangular lattice model, the approach to the thermodynamic limit is found to be algebraic with the system size M. We will not give details of these calculations in this paper. Rather, we will focus upon the scaling behavior in the critical region.

Three different lattice shapes for the K model are considered in this paper: (1) shape $N\times\infty$, in which the lattice has $2N$ lattice sites in the horizontal x direction but is infinite in the vertical y direction, (2) shape $\infty\times M$, in which the lattice has $2M$ lattice sites in the vertical y direction but is infinite in the horizontal x direction, and (3) the general shape $N\times M$ in which the lattice is finite

in both directions with $2M$ lattice sites in the vertical direction and $2N$ lattice sites in the horizontal direction. Since we are interested in the finite-size effect, periodic boundary conditions in the two principal lattice directions will be used throughout this paper. Periodic boundary conditions and the choice of the unit cell in Fig. 2(a) (to be used in the Pfaffian solution) demands that the number of lattice sites in each direction be even. The behavior of the specific heat for shapes $N\times\infty$ and $\infty\times M$ are studied in Secs. III and IV. Finite-size-scaling theory is shown to be valid and the scaling variables are identified for these two shapes. From these results it becomes clear that the relevant shape factor is $\kappa=N^2/M$. (In previous calculations on the rectangular lattice dimer model[24] and the Ising model[25] the relevant shape factor was $\delta=N/M$ because of the obvious equivalence of the x and y axes.) To verify this new shape dependence the thermodynamic limit is calculated in Sec. V for lattice sizes finite in both directions at fixed values of κ. In Sec. VI the results for the three different shapes are compared and shown to follow a consistent pattern. From this pattern and the identification of the scaling variables the values of ν_x and ν_y are determined and conclusions are drawn in Sec. VII. Section II begins with the relevant formulas and notations for subsequent calculations.

II. FUNDAMENTAL FORMULAS AND NOTATIONS

It is well known[1,6] that the partition function Z for a planar dimer model with periodic boundary conditions can be expressed as a linear combination of four Pfaffians. A straightforward extension of the standard method as presented by McCoy and Wu in Ref. 6 for the rectangular lattice model gives the Pfaffians for the generalized K model of Fig. 2(a) (see also Ref. 11). By setting $y=0$, the partition function of the K model of size $2N\times 2M$ is[27]

$$Z=\frac{1}{2}\sum_{j=1}^{4} Z_j \,, \tag{2.1}$$

where

$$Z_j=\Upsilon_j \prod_{n=1}^{N}\prod_{m=1}^{M} |g(\phi_1,\phi_2)| \,, \tag{2.2}$$

$$\Upsilon_j=\begin{cases} -1 & \text{if } j=1 \\ 1 & \text{otherwise} \,, \end{cases} \tag{2.3}$$

$$g(\phi_1,\phi_2)=2x^2(1-\cos\phi_1)-\exp(i\phi_2) \,, \tag{2.4}$$

$$x=\exp(-\beta\epsilon) \,, \tag{2.5}$$

$$\phi_1=\begin{cases} \pi\dfrac{2n}{N} & \text{for } j=1 \text{ and } 2 \\ \pi\dfrac{2n-1}{N} & \text{for } j=3 \text{ and } 4 \,, \end{cases} \tag{2.6}$$

and

$$\phi_2=\begin{cases} \pi\dfrac{2m}{M} & \text{for } j=1 \text{ and } 3 \\ \pi\dfrac{2m-1}{M} & \text{for } j=2 \text{ and } 4 \,. \end{cases} \tag{2.7}$$

The allowed sets of values of ϕ_1 and ϕ_2 can be recognized as the components of the reciprocal vectors of a lattice of size $N\times M$. Note that N and M correspond to the number of unit cells in the two directions and also note that the physics of the system does not depend crucially upon whether N and M are odd or even. However, to avoid dealing with two separate cases in the following sections we will take N to be even; the asymptotic scaling functions do not depend upon this choice.

Since from Eq. (2.7) $\exp\{i\phi_2(m)\}$ are the Mth roots of ± 1, the product over m can be performed to reduce the right-hand side (rhs) of Eq. (2.2) to a single product over n. The factors in the resulting product are of the type $\{2x\sin(\phi_1/2)\}^{2M}\pm 1$ and the product is taken over the allowed values of ϕ_1 given by Eqs. (2.6) and (2.2). One can use the symmetry of the trigonometric function about $\pi/2$ to reduce the number of factors to $N/2$ because every $n<N/2$ in Eq. (2.6) can be paired with an $n>N/2$, except when $n=N$ and $n=N/2$ for $j=1$ and 2. For $n=N$, and $j=1$ and 2, $\phi_1=2\pi$ so that $2x\sin(\phi_1/2)=0$ giving a contribution of $(-1)^j$ to the product. We combine this factor with Υ_j in Eq. (2.3) so as to yield a positive contribution for all j. Introducing the notations

$$s(\phi)=2x\cos\phi \,, \qquad p=N/2 \,, \tag{2.8}$$

we have

$$Z_j=\begin{cases} [(-1)^j+(2x)^{2M}]\displaystyle\prod_{n=1}^{p-1}[(s(n\pi/N))^{2M}+(-1)^j]^2 & \text{if } j=1 \text{ and } 2 \qquad (2.9) \\ \displaystyle\prod_{n=1}^{p}\{[s((n-\tfrac{1}{2})\pi/N)]^{2M}+(-1)^j\}^2 & \text{if } j=3 \text{ and } 4 \,. \qquad (2.10) \end{cases}$$

For later convenience we have used the cosine function in Eq. (2.8). The factor outside the product sign in Eq. (2.9) corresponds to $\phi_1=\pi$ in Eq. (2.6) which is equivalent to $\phi=0$ in Eq. (2.8) since $\phi=(\pi-\phi_1)/2$.

The fundamental thermodynamic relation $4MNf=-k_BT\ln Z$ connects the free energy per lattice site, f, to the partition function Z. The density of horizontal dimers, ρ, is determined by

$$4MN\rho=x\frac{d}{dx}\ln Z \tag{2.11}$$

and the specific heat per lattice site, $c_{N\times M}(T)$, is given by the derivative of the energy density ($=\epsilon\rho$) with respect to temperature. Denoting the differentiation with respect to x by a prime and using the notations

$$E_j=\frac{1}{Z_j}xZ_j' \quad \text{and} \quad C_j=\frac{1}{Z_j}x(xZ_j')'-\left[\frac{1}{Z_j}xZ_j'\right]^2 \quad \text{for } j=1,2,3,4\ , \tag{2.12}$$

it is convenient to write

$$4MNc_{N\times M}(T)=\frac{\epsilon}{x}\frac{dx}{dT}\left[\frac{\sum_j Z_j(C_j+E_j^2)}{\sum_j Z_j}-\left[\frac{\sum_j Z_jE_j}{\sum_j Z_j}\right]^2\right]. \tag{2.13}$$

In the thermodynamic limit ($N,M\to\infty$), the density of horizontal dimers, $\rho(T)$, and the specific heat $c_{\infty\times\infty}(T)$ are given by[1,2]

$$\rho(T)=c_{\infty\times\infty}(T)=0 \quad \text{if } x\le\tfrac{1}{2}\ , \tag{2.14}$$

and, if $x>\frac{1}{2}$,

$$\rho(T)=\frac{1}{\pi}\cos^{-1}\left[\frac{1}{2x}\right] \tag{2.15}$$

and

$$c_{\infty\times\infty}(T)=(k_B/\pi)(\ln x)^2(4x^2-1)^{-1/2}\ . \tag{2.16}$$

These equations show that the thermodynamic functions are nonanalytic at $x_c=\frac{1}{2}$. The variable $4x^2-1$ in Eq. (2.16) will appear repeatedly in subsequent sections. This variable is related asymptotically to the reduced temperature $t\equiv(T-T_c)/T_c$, as one can easily see by recalling that $x=\exp(-\beta\epsilon)$ and $x_c=\frac{1}{2}$. Then, Eq. (2.16) explicitly exhibits the $t^{-1/2}$ dependence of the bulk specific heat as $t\to 0+$. Equation (2.15) shows that $\rho(T)$, which is the inverse of the average separation of the domain walls in Fig. 1, vanishes with an exponent $\frac{1}{2}$ as $T\to T_c+$. This result, though known for a long time, has recently been rediscovered in the context of domain wall models.[28] Our task in the following sections is to evaluate the asymptotic forms of the sums and the products appearing in Eqs. (2.9), (2.10), (2.12), and (2.13) as N and M approach infinity.

III. LATTICES OF SHAPE $N\times\infty$

The thermodynamic limit of infinite lattice size can be taken in many different ways since both N and M must go to infinity. In this section we will first let $M\to\infty$ so that the lattice becomes infinite in the vertical direction while remaining finite in the horizontal direction with $2N$ lattice points and N unit cells. Such semi-infinite lattices will be called $N\times\infty$ lattices. For lattices of size $N\times\infty$ the K model is known to exhibit a sequence of first-order transitions.[17] (This property has been used to study the critical behavior[17] of a three-dimensional analog[29] of the two-dimensional K model.) In this section we derive these transition temperatures for the K model. This will enable us to exhibit an explicit finite-size-scaling form which identifies the appropriate scaling variable when the final limit $N\to\infty$ is taken.

The origin of the sequence of first-order transitions in the K model of size $N\times\infty$ can be understood in a simple way if one thinks of the excited states above the ground state. As discussed in the Introduction each first excited state has one horizontal dimer in each row of the lattice. Since a horizontal dimer can be placed in two different ways in each row, the free energy per lattice site for this set of excited states is $(\epsilon-k_BT\ln 2)/(2N)$. Hence the set of first excited states will be thermodynamically preferred to the ground state if and only if $k_BT>k_BT_c=\epsilon/\ln 2$. This simple argument actually locates the bulk critical temperature exactly. The transition from the ground state to the set of first excited states is a first-order transition because the energy density of this finite system changes discontinuously from 0 to $\epsilon/(2N)$. In the same fashion, another first-order transition takes place when the set of second excited states, with two horizontal dimers per row, is preferred to the set of first excited states. Such transitions continue to occur as the temperature is increased until the system becomes maximally disordered. In the limit $N\to\infty$ these transition temperatures form a dense set and their density determines the bulk behavior.[26]

The above sequence of transition temperatures can be calculated exactly from Eqs. (2.9) and (2.10). First we consider the region where $2x<1$. Then $s^{2M}(\phi)$ in Eqs. (2.9) and (2.10) vanishes in the limit $M\to\infty$ because $s(\phi)$ in Eq. (2.8) is less than one for all ϕ. Therefore $Z=(-1+1+1+1)/2=1$ for all $T<T_c$, where T_c is determined by $x_c=\frac{1}{2}$. This means that the system remains frozen in the ground state for all $T<T_c$ with zero free energy. However as T is increased above T_c ($2x>1$), $s(\phi)$ can be greater than 1. If the temperature is such that $s(\phi=0)>1$ but $s(\phi)<1$ for all other allowed values of ϕ in Eqs. (2.9) and (2.10), then only the pair Z_1 and Z_2 survive the limiting procedure ($M\to\infty$), each being equal to $(2x)^{2M}$. This yields

$$Z=(2x)^{2M} \tag{3.1}$$

or, equivalently,

$$f_{N\times\infty}(T)=-\frac{k_BT}{2N}\ln(2x)\ . \tag{3.2}$$

The energy density, obtained by taking the appropriate derivative of $\ln Z$, is now $\epsilon/(2N)$, i.e., the system is now in the first excited state, showing that the first transition has taken place at the bulk critical point $x=\frac{1}{2}$, just as predicted by the simple argument in the preceding paragraph. The system remains frozen in this state, as the

temperature is changed, until another $s(\phi)$ becomes greater than 1. From Eq. (2.8) we see that the next term in the queue to cross the barrier is the $n=1$ term of Z_3 and Z_4. However this crossing does not alter the partition function as long as $s(0)>(s(\pi/2N))^2$ because $Z_{1,2}\gg Z_{3,4}$, and so the free energy after summing in Eq. (2.1) is still given by Eq. (3.2). But as T is increased further $(s(\pi/2N))^2$ can become greater than $s(0)$, so the partition function is dominated by $Z_{3,4}$ and the free energy per lattice site is given by

$$f_{N\times\infty}(T)=-\frac{k_BT}{2N}2\ln\left[2x\cos\left[\frac{\pi}{2N}\right]\right]. \tag{3.3}$$

The energy density is now ϵ/N showing that the second transition has taken place at a temperature T_2, determined by

$$2x\cos^2(\pi/2N)=1\,. \tag{3.4}$$

This "survival of the stronger term" argument can be used repeatedly to locate the other transition temperatures. Denoting the transition temperatures by T_i, with $i=2,3,\ldots,$ one can see that the odd values of i correspond to jumps from the pair $Z_{3,4}$ to the pair $Z_{1,2}$ while the reverse jumps are responsible for the T_i's with even values of i. The activities x_i that correspond to these transition temperatures are given by

$$2x_i=\left[\left[\prod_{j=0}^{q-1}\cos^2\left[\frac{j\pi}{N}\right]\right]\left[\prod_{j=1}^{q}\cos^2\left[\frac{(2j-1)\pi}{2N}\right]\right]\right]^{-1} \quad \text{if } i \text{ is even}, \tag{3.5}$$

$$2x_i=\left[\left[\prod_{j=1}^{q}\cos^2\left[\frac{(2j-1)\pi}{2N}\right]\right]\left[\prod_{j=0}^{q}\cos^2\left[\frac{j\pi}{N}\right]\right]\right]^{-1} \quad \text{if } i \text{ is odd and greater than 1}, \tag{3.6}$$

where $q=[i/2]_i$, the integer part of $i/2$. For the first transition at T_1 $(=T_c)$, we have $2x_1=1$. For finite i, expanding the cosine functions in Eqs. (3.5) and (3.6), one can show that the activities x_i's have the following asymptotic behavior:

$$N^2(4x_i^2-1)\approx\tfrac{1}{4}\pi^2 i(i-1) \quad \text{with } i=1,2,\ldots, \tag{3.7}$$

up to $O(N^{-2})$ as $N\to\infty$. Note that the rhs of Eq. (3.7) is independent of N. The above equation (3.7) also shows that when the limit $N\to\infty$ is taken all the transition temperatures approach[17] the bulk critical temperature T_c as N^{-2}.

Between any two successive transition temperatures the $N\times\infty$ system remains frozen in a set of excited states, and so the specific heat is identically zero except at the sequence of first-order transition temperatures. Therefore, the specific heat per lattice site can be written as a sum of delta functions

$$c_{N\times\infty}(T)=\frac{\epsilon}{2N}\sum_i\delta(T-T_i) \tag{3.8}$$

which, by changing over to the activity x, becomes

$$c_{N\times\infty}(T)=\frac{k_B}{2N}x(\ln x)^2\sum_i\delta(x-x_i)\,. \tag{3.9}$$

We now perform a few elementary manipulations to exhibit the specific heat in finite-size-scaling form. One has

$$x-x_i=\tfrac{1}{2}((2x-1)-(2x_i-1))$$

$$\approx\frac{1}{4N^2}(N^2(4x^2-1)-N^2(4x_i^2-1)) \tag{3.10}$$

asymptotically in the limit $N\to\infty$ and x close to x_c because in this limit, by Eq. (3.7), the x_i's also approach $x_c=\frac{1}{2}$. Defining

$$\tau_N=N^2(4x^2-1) \tag{3.11}$$

and using the property $\delta(ax)=a^{-1}\delta(x)$, the asymptotic form of Eq. (3.9) is

$$c_{N\times\infty}(t)\approx k_BN\mathscr{P}(\tau_N,0)\,, \tag{3.12}$$

where, using Eq. (3.7)

$$\mathscr{P}(\tau_N,0)=(\ln 2)^2\sum_i\delta(\tau_N-\pi^2i(i-1)/4)\,. \tag{3.13}$$

The significance of the second variable with the value zero in the scaling function $\mathscr{P}(\tau_N,0)$ will be revealed in Sec. VI. Equation (3.12) is in the scaling form of Eq. (1.1) with $\omega_N=1$ and $\nu_N=1/2$, even though the scaling function $\mathscr{P}(\tau_N,0)$ is a highly nonanalytic function.

IV. LATTICES OF SHAPE $\infty\times M$

In this section the infinite limits are taken in reverse order compared to the previous section. First, the limit $N\to\infty$ of lattice sites in the horizontal direction is taken. This gives a semi-infinite lattice that will be described as an $\infty\times M$ lattice where M is the finite number of unit cells (i.e., with $2M$ lattice sites) in the vertical direction. For this type of semi-infinite lattices the energy gaps, unlike the previous case, are not infinite. Such finite energy excitations essentially make each of these lattices into typical one-dimensional models that cannot have a phase transition and so all the thermodynamic quantities are smooth analytic functions of temperature except in the thermodynamic limit as $M\to\infty$. Again we show that close to the critical point the specific heat per lattice site can be written in the finite-size-scaling form of Eq. (1.1). The free energy can also be written in a scaling form,[26] but as it does not give any additional information we will concentrate only on the specific heat in this paper.

Since N is infinite, the difference between the products in Eq. (2.2), for the two allowed sets of angles in Eq. (2.6), is negligible so that Z_1 cancels Z_3 (see Appendix A for

details). Therefore, the partition function for the $\infty \times M$ lattice has the following form:

$$\lim_{N\to\infty}\left[\frac{\pi}{2N}\ln Z\right]=\int_0^{\pi/2}\ln(1+(2x\cos\phi)^{2M})d\phi \tag{4.1}$$

and the specific heat per lattice site is given by

$$c_{\infty\times M}(T)=k_B\frac{2M}{\pi}(\ln x)^2\int_0^{\pi/2}\frac{(2x\cos\phi)^{2M}}{[1+(2x\cos\phi)^{2M}]^2}d\phi\ . \tag{4.2}$$

For $x<\frac{1}{2}$, the rhs of Eq. (4.1) is less than $b\ln(1+(2x)^{2M})$ for some constant b independent of M, so that the free energy

$$f_{\infty\times M}\sim O(\exp[2M\ln(2x)]) \tag{4.3}$$

as $M\to\infty$. This shows that at a fixed temperature below T_c the free energy approaches its thermodynamic limit of zero exponentially fast. If, however, the thermodynamic limit is taken in such a way that $M\ln(2x)\sim M(4x^2-1)$ is $O(1)$, for x close to $x_c=\frac{1}{2}$, the approach is no longer exponential. In other words the thermodynamic limit is not achieved in a region close to x_c and the critical region is determined by the variable

$$\tau_M=M(4x^2-1)\ . \tag{4.4}$$

The analysis for a fixed $x>\frac{1}{2}$ involves a more detailed calculation because $s(\phi)$ [defined in Eq. (2.8)] is no longer less than one for all values of ϕ. In this paper we will not describe this more lengthy analysis which shows that the same variable τ_M determines the critical region on the high-temperature side also. However, strong numerical evidence to support this assertion will be presented.

We now study the limiting behavior of the thermodynamic quantities as $M\to\infty$ for a fixed τ_M. The temperature appears in Eqs. (4.1) and (4.2) in the form $(2x)^{2M}$ so that

$$(2x\cos\phi)^{2M}=\exp(\tau_M+2M\ln\cos\phi)+O(M^{-1}) \tag{4.5}$$

as $M\to\infty$. The two temperature regions $T<T_c$ and $T>T_c$ are considered separately because of the difference in the behavior of $s(\phi)$ for the two cases.

A. $T<T_c$

For $T<T_c$, τ_M in Eq. (4.4) is negative and the argument of the exponential in Eq. (4.5) is monotonically decreasing with ϕ in the entire range 0 to $\pi/2$. Therefore, $(2x\cos\phi)^{2M}$ is less than one and the denominator of the integral in Eq. (4.2) can be expanded as a convergent series,

$$I=\sum_{r=1}^{\infty}(-1)^r rJ_r\ , \tag{4.6}$$

where

$$J_r=\exp(\tau r)\int_0^{\pi/2}\exp(2Mr\ln\cos\phi)d\phi\ . \tag{4.7}$$

Because of the monotonic behavior of the integrand in Eq. (4.7), the leading contribution in the asymptotic limit comes from a region close to $\phi=0$. One can use the first term of the expansion

$$\ln\cos\phi=-\tfrac{1}{2}\phi^2-\tfrac{1}{12}\phi^4+\cdots \tag{4.8}$$

to approximate the integrand. The range of integration can also be extended to infinity. The errors from each of these two steps can be estimated to show that they are less significant (see Appendix B for details) than the leading term which is

$$\exp(\tau r)\int_0^{\infty}\exp(-rM\phi^2)d\phi\ . \tag{4.9}$$

By changing the integration variable to $s=M^{1/2}\phi$ we have

$$J_r\approx M^{-1/2}\int_0^{\infty}\exp(r(\tau-s^2))ds\ . \tag{4.10}$$

Putting the above asymptotic form for J_r in Eq. (4.10) into Eq. (4.6) and thence into Eq. (4.2) we obtain

$$c_{\infty\times M}(t)=\mathscr{P}(\tau_M,\infty)M^{1/2}+O(M^{-1/2})\ , \tag{4.11}$$

where

$$\mathscr{P}(\tau_M,\infty)=\frac{2(\ln 2)^2}{\pi}\int_0^{\infty}\frac{\exp(\tau_M-s^2)}{(1+\exp(\tau_M-s^2))^2}ds\ . \tag{4.12}$$

Although the derivation assumes $\tau_M<0$, we will see shortly that Eq. (4.12) is also valid for $\tau_M\geq 0$. The meaning of the value infinity of the second variable in the scaling function in Eq. (4.12) will be revealed in Sec. VI. Also, to obtain Eq. (4.12), we have replaced $\ln x$ by $(-\ln 2)$, because x approaches 1/2 for a fixed τ_M as $M\to\infty$.

B. $T>T_c$

For $T>T_c$, $\tau+2M\ln\cos\phi$ in Eq. (4.5) will be positive for

$$\cos\phi>\cos\phi_0\equiv\exp(-\tau_M/(2M))\ . \tag{4.13}$$

To evaluate the integral I in Eq. (4.2), we now break it up into two parts as

$$I=I_1+I_2\ , \tag{4.14}$$

where

$$I_1=\int_0^{\phi_0}\frac{(2x\cos\phi)^{-2M}}{(1+(2x\cos\phi)^{-2M})^2}d\phi\ , \tag{4.15}$$

and

$$I_2=\int_{\phi_0}^{\pi/2}\frac{(2x\cos\phi)^{2M}}{(1+(2x\cos\phi)^{2M})^2}d\phi\ , \tag{4.16}$$

so that the denominator of each integrand is of the form $1+z$ with $z<1$. The denominators of $I_{1,2}$ can now be expanded to obtain integrals like J_r in Eq. (4.7), with appropriate limits and with the replacement of M by $-M$ for I_1. For both $I_{1,2}$, the leading contributions come from a region close to $\phi=\phi_0$, where one has

$$\ln\cos\phi = -\frac{\tau_M}{2M} - (\exp(\tau_M/M)-1)^{1/2}(\phi-\phi_0)$$

$$-\frac{1}{2}(\exp(\tau_M/M))(\phi-\phi_0)^2+\cdots . \quad (4.17)$$

As was done in Sec. IV A for $T<T_c$, one can use Eq. (4.17) to simplify the integrands of $I_{1,2}$. The errors introduced by doing so can be estimated along the same lines sketched in Appendix B. By changing the integration variable to $\phi-\phi_0$, one limit of each integral ($I_{1,2}$) can be made zero. The upper limit for I_2 can be extended to infinity, as in Eq. (4.9), giving

$$I_2 \approx M^{-1/2}\int_0^\infty \frac{\exp(-2\tau_M^{1/2}s-s^2)}{(1+\exp(-2\tau_M^{1/2}s-s^2))^2}ds . \quad (4.18)$$

However, the range of integration for I_1 cannot be extended to infinity because ϕ_0 decreases to 0 as

$$\phi_0=(\tau_M/M)^{1/2}+O(M^{-3/2}) \quad (4.19)$$

as $M\to\infty$. The change of variable to $s=-M^{1/2}(\phi-\phi_0)$ gives the lower limit of I_1 to be $\tau_M^{1/2}$. Therefore,

$$I_1 \approx M^{-1/2}\int_0^{\tau_M^{1/2}} \frac{\exp(-2\tau_M^{1/2}s+s^2)}{(1+\exp(-2\tau_M^{1/2}s+s^2))^2}ds . \quad (4.20)$$

The details of the error estimates are omitted. The leading contribution to the specific heat is obtained by combining Eqs. (4.18), (4.20), (4.14), and (4.2) giving

$$c_{\infty\times M}(t)=k_B\mathscr{P}(\tau_M,\infty)M^{1/2}+O(M^{-1/2}) , \quad (4.21)$$

where

$$\mathscr{P}(\tau_M,\infty)=\frac{2(\ln 2)^2}{\pi}\left[\int_0^\infty \frac{\exp(-2\tau_M^{1/2}s-s^2)}{(1+\exp(-2\tau_M^{1/2}s-s^2))^2}ds+\int_0^{\tau_M^{1/2}} \frac{\exp(-2\tau_M^{1/2}s+s^2)}{(1+\exp(-2\tau_M^{1/2}s+s^2))^2}ds\right] \quad (\tau_M>0) . \quad (4.22)$$

Equation (4.22) is the analytic continuation of Eq. (4.12). This can easily be verified by completing the squares in the arguments of the exponentials in the two integrands of Eq. (4.22) and changing the integration variables appropriately. This proves that the scaling function $\mathscr{P}(\tau_M,\infty)$ given by Eq. (4.12) is valid for both $\tau_M<0$ and $\tau_M\geq 0$.

C. The scaling functions

We have shown that for an $\infty\times M$ lattice, the specific heat close to T_c can be expressed in a scaling form

$$c_{\infty\times M}(t)\approx k_B\mathscr{P}(\tau_M,\infty)M^{1/2} , \quad (4.23)$$

where the scaling function $\mathscr{P}(\tau_M,\infty)$ is given by Eq. (4.12) for $\tau_M<0$ and by Eq. (4.22) for $\tau_M>0$. The scaling function $\mathscr{P}(\tau_M,\infty)$ depends solely on the scaled variable $\tau_M=M(4x^2-1)\sim Mt$ and not on M and x separately, consistent with Eq. (1.1). The finite-size exponents are therefore given by $\omega_M=1/2$ and $\nu_M=1$ for $\infty\times M$ lattices.

The scaling function $\mathscr{P}(\tau_M,\infty)$ has been plotted in Fig. 5 (solid line) as a function of τ_M; this calculation involves numerical integration of Eq. (4.12), using a standard International Mathematical and Statistical Library (IMSL) routine,[30] to an absolute error of 1 in 10^5. From Eqs. (4.12) and (4.22), and Fig. 5 it follows that $\mathscr{P}(\tau_M,\infty)$ is a monotonically decreasing function of $|\tau_M|$ for $\tau_M<0$ but first increases to a maximum for positive values of τ_M. Therefore, the reduced pseudocritical temperature t_m [Eq. (1.3)] is positive for this shape. The maximum of $\mathscr{P}(\tau_M,\infty)$ is found to occur at $\tau_{\max}=1.108$. Translated into ordinary temperature, this means

$$t_m\approx 0.7993/M \quad (4.24)$$

as $M\to\infty$. Therefore the shift exponent λ is 1 and the amplitude $b=0.7993$ [see Eq. (1.3)].

One can check from Eqs. (4.12) and (4.22) that $\mathscr{P}(\tau_M,\infty)\to((\ln 2)^2/\pi)\tau_M^{-1/2}$ as $\tau_M\to+\infty$ and $\mathscr{P}(\tau_M,\infty)\sim\exp(-|\tau_M|)$ as $\tau_M\to-\infty$. When these limiting forms are used in Eq. (4.23), one obtains the bulk behavior of Eq. (2.16). This is a requirement the scaling function has to satisfy and, as discussed in the Introduction, it predicts $\omega_M=\alpha/\nu_M$ which is consistent with our result of $\omega_M=1/2$ because $\alpha=1/2$ for the K model.[1] Since the finite-size-scaling theory is found to hold with the same exponents on the two sides of T_c and since the scaling function approaches zero as τ_M approaches $-\infty$, one can interpret the asymmetric bulk behavior of the specific heat [Eqs. (2.14) and (2.16)] as $\alpha=\alpha'=1/2$ with zero amplitude on the low-temperature side.

D. Comparison of the asymptotic form with direct numerical evaluation

The specific heat for a given value of M has been computed by numerically integrating Eq. (4.2) using the stan-

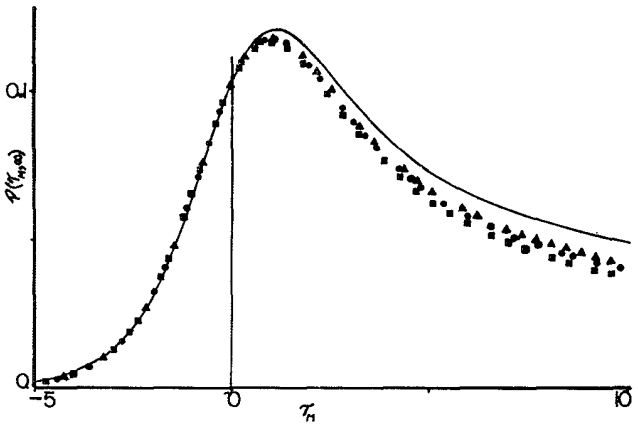

FIG. 5. Plot of the scaling function $\mathscr{P}(\tau_M,\infty)$ for shape $\infty\times M$ (Sec. IV) vs $\tau_M=M(4x^2-1)\sim Mt$. The numerically calculated points from Eq. (4.2) are: (i) ■ for $M=50$, (ii) ● for $M=70$, and (iii) ▲ for $M=90$.

dard IMSL routine.[30] These numerical results for different values of M are plotted against the variable τ_M in Fig. 5 to compare with our asymptotic results. Note the spectacular collapse of the calculated points on the solid curve for $T<T_c$ indicating that the error in using Eq. (4.23) is negligible for $M\sim 50$. In contrast, for $T>T_c$, the numerical results for finite M clearly differ from the asymptotic scaling form but they systematically approach the solid curve. To show that for $\tau_M>0$ the specific heat for these semi-infinite systems really approaches the solid curve in Fig. 5 in the asymptotic limit, the quantity $M^{-1/2}c_{\infty\times M}(t)$ has been calculated for different values of M keeping τ_M fixed at $\tau_M=0$ and $\tau_M=2$. The numerical values obtained are then plotted against $1/M$ in Fig. 6 [curves a and b] and extrapolated to the $1/M=0$ limit. These extrapolated values agree remarkably well with $\mathscr{P}(0,\infty)=0.103\,03$ and $\mathscr{P}(2,\infty)=0.113\,35$ obtained from Eq. (4.12). Curve c in the same figure shows a similar extrapolation plot for the maximum specific heat, computed from Eq. (4.2), and the extrapolated value is found to agree with $\mathscr{P}(\tau_{\max},\infty)=0.120\,98$. The extrapolated value for the amplitude b (for t_m), obtained from curve d where numerically calculated values of Mt_m are plotted against $1/M$, is also found to agree with the value given in Eq. (4.24).

The agreement between the extrapolated numerical values in Fig. 6 with the values from our asymptotic scaling function provides strong numerical support that τ_M is the proper scaling variable in the high-temperature region for $\infty\times M$ lattices. Let us consider a general form $M^\theta t$ for the scaling variable so that for a fixed $\tau_M\sim Mt$, the scaling function would behave as $\mathscr{P}(M^{\theta-1}\tau_M)$. Now in the limit $M\to\infty$ there are three possibilities: (1) $\lim_{M\to\infty}\mathscr{P}(M^{\theta-1}\tau_M)=\mathscr{P}(0)$ for all τ_M if $\theta<1$, (2) $\lim_{M\to\infty}\mathscr{P}(M^{\theta-1}\tau_M)=\mathscr{P}(\infty)$ for all τ_M if $\theta>1$, and (3) $\lim_{M\to\infty}\mathscr{P}(M^{\theta-1}\tau_M)=\mathscr{P}(\tau_M)$ if $\theta=1$. In the first two cases the limits are independent of τ_M. However, the extrapolations in Fig. 6 strongly indicate that the limiting values depend on τ_M. This dependence on τ_M is inconsistent with the first two possibilities and supports the conclusion that $\nu_M=1$ and that τ_M is the proper scaling variable.

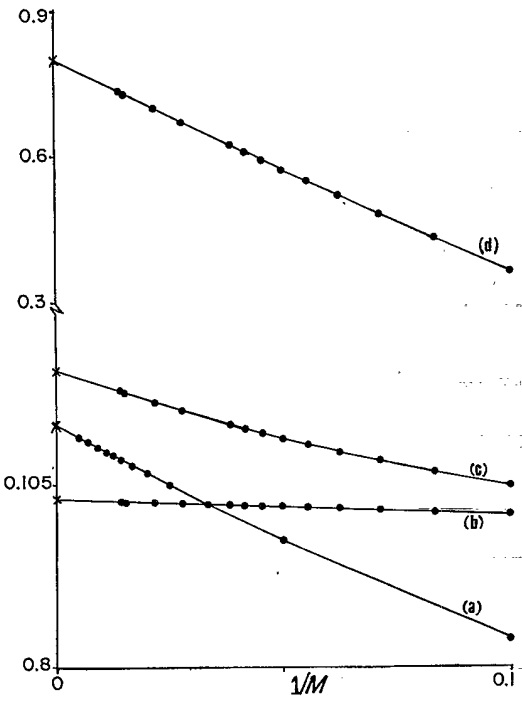

FIG. 6. $1/M$ extrapolation plots using numerically calculated specific heats from equation (4.2). (a) $M^{-1/2}c_{\infty\times M}(T)$ with $\tau_M=2$, (b) $M^{-1/2}c_{\infty\times M}(T_c)$, i.e., with $\tau_M=0$. (c) $M^{-1/2}c_{\infty\times M}(T_m)$, where T_m is the temperature for maximum specific heat and (d) Mt_m for the reduced pseudocritical temperature. [Note the change in scale for curve (d).] Asymptotic values computed from Fig. 5 are shown by $\times$'s on the vertical axis. These are respectively $\mathscr{P}(2,\infty)$, $\mathscr{P}(0,\infty)$, $\mathscr{P}(\tau_{\max},\infty)$, and b [see Eq. (4.24)].

V. LATTICES OF SHAPE $N\times M$

The results of the preceding two sections emphasize the strong dependence of the scaling functions and the scaling variables upon the order of taking the infinite size thermodynamic limit of the lattice. At first glance it would appear that the scaling function for $N\times\infty$ lattice shapes is completely unconnected with the scaling function for $\infty\times M$ lattice shapes. In fact there is an underlying unity which, however, can only emerge if a shape variable is explicitly considered. In this section consideration of general lattices of shape $N\times M$ reveals what the appropriate shape variable κ is. It might be noted that the shape variable $s=N/M$ which was appropriate for isotropic Ising and dimer models, is *not* appropriate for the K model. Calculations,[26] which we will not give here, show that taking the thermodynamic limit holding s constant always reduces to the scaling function derived for $\infty\times M$ lattices in Sec. IV. This section also derives the formulas from which the unified scaling function can be computed for arbitrary values of κ.

First we note that the partial partition functions Z_j in Eqs. (2.9) and (2.10) involve $\exp(2M\ln s(\phi))$ which for $x<1/2$ leads to an exponential approach to the thermodynamic limit as we have seen in Eq. (4.3). This shows that τ_M defines the critical region for finite systems also. From Eq. (2.9) we have

$$\ln Z_2=-\ln(1+(2x)^{2M})+2\sum_{n=0}^{p}\ln[1+(s(n\pi/N))^{2M}]\,. \tag{5.1}$$

For $x<1/2$, following the arguments of the previous section (Sec. IV A), one finds that the leading contribution to the sum on the rhs of the above equation comes from a region close to $n=0$. For $n\ll N$, we have

$$2M\ln\cos\left[\frac{\pi n}{N}\right]=-\frac{M}{N^2}(\pi n)^2-\frac{M}{N^4}(\pi n)^4+\cdots \tag{5.2}$$

showing that for a fixed τ_M, this n-dependent contribution becomes significant only if

$$\kappa=N^2/M \tag{5.3}$$

is held constant because only then is $s(n\pi/N)$ of $O(1)$. One comes to the same conclusion from the other three

partial partition functions. This identifies κ as the shape factor to be kept constant as the thermodynamic limit is taken.

For a fixed value of κ we have to evaluate all four terms in Eq. (2.1) and also the quantities defined in Eq. (2.12). The explicit forms of E_j and C_j are given below:

$$E_j=2M\sum_n \frac{s_j^{2M}(n)}{s_j^{2M}(n)+(-1)^j}=2M\mathscr{E}_j \tag{5.4}$$

and

$$C_j=(-1)^j(2M)^2\sum_n \frac{s_j^{2M}(n)}{[s_j^{2M}(n)+(-1)^j]^2}=(2M)^2\mathscr{C}_j\ , \tag{5.5}$$

where

$$s_j(n)=\begin{cases} s(n\pi/N) & \text{if } j=1 \text{ and } 2 \\ s((n-\frac{1}{2})\pi/N) & \text{if } j=3 \text{ and } 4\ . \end{cases} \tag{5.6}$$

The above two equations (5.4) and (5.5) define two new quantities $\mathscr{E}_j$ and $\mathscr{C}_j$. Using these in Eq. (2.13), one finds

$$c_{N\times M}(T)=k_B(\ln x)^2\frac{M}{N}\left[\frac{\sum_j Z_j(\mathscr{C}_j+\mathscr{E}_j^2)}{\sum_j Z_j}-\left[\frac{\sum_j Z_j\mathscr{E}_j}{\sum_j Z_j}\right]^2\right]. \tag{5.7}$$

Note, in particular, that for a fixed κ

$$M/N=\kappa^{-1/2}M^{1/2}=\kappa^{-1}N\ . \tag{5.8}$$

For later use we introduce a size-dependent variable $\mathscr{M}$ defined as

$$\mathscr{M}=\frac{\kappa}{1+\kappa}M=\frac{MN^2}{M+N^2} \tag{5.9}$$

so that

$$M/N=\mathscr{M}^{1/2}(1+\kappa)^{1/2}/\kappa\ . \tag{5.10}$$

The following analysis will show that the expression inside the big bracket in Eq. (5.7) is, in the thermodynamic limit, a function of τ_M and κ only so that in the scaling limit Eq. (5.8) or Eq. (5.10) gives the relevant M or N dependence for fixed values of τ_M and κ. This analysis is performed separately below for $T<T_c$ and $T>T_c$.

A. $T<T_c$

Our results in Sec. IV make it clear that, for $x<1/2$, the leading contributions to the partial partition functions come from the values of $n\ll N$. For example, expanding the logarithm in the summand on the rhs of Eq. (5.1), for Z_2, we have to evaluate the following sum:

$$\sum_{l=1}^{\infty}\frac{(-1)^{l+1}}{l}S_l\ , \tag{5.11}$$

where

$$S_l=\sum_{n=1}^{p}\exp\left[l\tau_M+2\kappa M\ln\cos\left[\frac{n\pi}{N}\right]\right]. \tag{5.12}$$

Using Eq. (5.2), one approximates

$$S_l\approx\sum_{n=1}^{\infty}\exp\{l[\tau_M-(\pi n)^2/\kappa]\}\ , \tag{5.13}$$

where the error comes from using only the first term of Eq. (5.2) and also from extending the range of summation to infinity. Using Eq. (5.13) in Eq. (5.11) we obtain the leading behavior of the partial partition function Z_j. The error estimates are performed in Appendix C to show that the error in $\ln Z_j$ is $O(N^{-1+\eta})$ with $\eta<1$. Similar analyses can be performed for the remaining Z_j, and for the $\mathscr{E}_j$ and $\mathscr{C}_j$. Defining

$$\mathscr{A}_j(n)=\begin{cases} \exp(\tau_M-(\pi n)^2/\kappa) & \text{for } j=1,2, \\ \exp[\tau_M-(\pi(n-\frac{1}{2}))^2/\kappa] & \text{for } j=3,4 \end{cases} \tag{5.14}$$

and representing the leading terms by a subscript 0, we have

$$\ln Z_{j,0}=2\left[\sum_{n=1}^{\infty}(\mathscr{A}_j(n)+(-1)^j)\right]+\begin{cases}((-1)^j+\exp(\tau_M)) & (j=1,2)\\ 1 & (j=3,4)\,,\end{cases} \tag{5.15}$$

$$\mathscr{C}_{j,0}-2\sum_{n=1}^{\infty}\frac{\mathscr{A}_j(n)}{\mathscr{A}_j(n)+(-1)^j}=\begin{cases}\dfrac{\exp(\tau_M)}{(-1)^j+\exp(\tau_M)} & (j=1,2)\\ 0 & (j=3,4)\,,\end{cases} \tag{5.16}$$

and

$$\mathscr{C}_{j,0}-2(-1)^j\sum_{1}^{\infty}\frac{\mathscr{A}_j(n)}{[\mathscr{A}_j(n)+(-1)^j]^2}=\begin{cases}(-1)^j\dfrac{\exp(\tau_M)}{[(-1)^j+\exp(\tau_M)]^2} & (j=1,2)\\ 0 & (j=3,4)\,.\end{cases} \tag{5.17}$$

B. $T>T_c$

For $T>T_c$, we make use of the angle ϕ_0 defined in Eq. (4.13). Since the summation in, say, Eq. (5.1) must be performed with integral values of the index, we define two quantities n_0' and n_0 as

$$\begin{aligned} n_0'&=N\phi_0/\pi\,,\\ n_0&=[n_0']_i\,,\end{aligned} \tag{5.18}$$

where $[n_0']_i$ is the integer part of n_0'. Then Z_2 in Eq. (2.9) may be written as

$$\ln Z_2=\ln(1+(2x)^{2M})+\sigma_1+\sigma_2+\sigma_3\,. \tag{5.19}$$

where

$$\sigma_1=2\sum_{n=1}^{n_0}\ln s_2(n)\,, \tag{5.20}$$

$$\sigma_2=2\sum_{n=1}^{n_0}\ln(1+s_2^{-2M}(n))\,, \tag{5.21}$$

and

$$\sigma_3=2\sum_{n=n_0+1}^{p}\ln(1+s_2^{2M}(n))\,, \tag{5.22}$$

s_2 being given by Eq. (5.6). The leading contributions to these σ_j's come from the neighborhood of $n=n_0$ and therefore Eq. (4.17), with appropriate values of ϕ, can be used to approximate these σ_j's. Since the procedure used for $T<T_c$ can be used again, a detailed discussion will not be given. For σ_3 a sum from 1 to infinity [compare with Eq. (4.14)] is obtained. This extension of the range of summation is not possible for $\sigma_{1,2}$ because asymptotically

$$n_0'=(\kappa\tau_M)^{1/2}/\pi+O(M^{-1}) \tag{5.23}$$

as $M\to\infty$ for a fixed κ, i.e., because n_0 is $O(1)$. One can still use Eq. (4.17) to obtain the asymptotic forms of $\sigma_{1,2}$, as in Eq. (4.20). Combining all the terms and changing the variable to $n=n-n_0$, the partial partition functions are given in the form of Eq. (5.15) where $\mathscr{A}_j$ has to be replaced by $\mathscr{B}_j$ defined as

$$\mathscr{B}_j(n)=\begin{cases}\exp\left[-2\pi\left[\dfrac{\tau_M}{\kappa}\right]^{1/2}(n-\kappa)-\dfrac{\pi^2}{\kappa}(n-\kappa)^2\right] & \text{if } j=1,2\\ \exp\left[-2\pi\left[\dfrac{\tau_M}{\kappa}\right]^{1/2}(n-\frac{1}{2}-\kappa)-\dfrac{\pi^2}{\kappa}(n-\frac{1}{2}-\kappa)^2\right] & \text{if } j=3,4\,,\end{cases} \tag{5.24}$$

where $\kappa=(\kappa\tau_M)^{1/2}/\pi-[(\kappa\tau_M)^{1/2}/\pi]_i$. The only major change needed there is the replacement of the lower limit of the sums from $n=1$ to $n=-\lambda$, where $\lambda=[(\kappa\tau_M)^{1/2}/\pi]_i-1$ and the term $n=0$ is to be excluded. Identical changes are also necessary to obtain $\mathscr{E}_{j,0}$ and $\mathscr{C}_{j,0}$ from Eqs. (5.16) and (5.17).

C. Final form

Combining the results of Secs. V A and V B with Eqs. (5.7) and (5.10), we obtain the final form for the specific heat per lattice site. We find that the leading term depends on two variables τ_M and κ. However, we prefer to write it in a slightly different form where the temperature dependent variable is taken as $\kappa\tau_M/(1+\kappa)$, for reasons to be explained in the next section. Therefore, we have

$$c_{N\times M}(t)\approx k_B\mathscr{P}(\kappa\tau_M/(1+\kappa),\kappa)\mathscr{M}^{1/2}, \tag{5.25}$$

where

$$\mathscr{P}(\kappa\tau_M/(1+\kappa),\kappa)=(\ln 2)^2\frac{(1+\kappa)^{1/2}}{\kappa}\left[\frac{\sum_j Z_{j,0}(\mathscr{C}_{j,0}+\mathscr{B}_{j,0}^2)}{\sum_j Z_{j,0}}-\left[\frac{\sum_j Z_{j,0}\mathscr{B}_{j,0}}{\sum_j Z_{j,0}}\right]^2\right] \tag{5.26}$$

with $Z_{j,0}$, $\mathscr{B}_{j,0}$, and $\mathscr{C}_{j,0}$, given by Eqs. (5.15)–(5.17) for $\tau_M\le 0$. For $\tau_M\ge 0$ one substitutes $\mathscr{B}_j$ from Eq. (5.24) into Eqs. (5.15)–(5.17) with the corresponding change in the lower limit of the summations as mentioned after Eq. (5.24).

Figure 7 shows the behavior of the scaling function $\mathscr{P}(\kappa\tau_M/(1+\kappa),\kappa)$ for $\kappa=1$ (solid line) as a function of $\tau_M/2$. The values of the specific heat calculated from Eq. (2.13) for small lattices with $\kappa=1$ are also shown there for comparison. The systematic approach in Fig. 7 of the exact finite lattice results to the scaling function $\mathscr{P}$ as the lattice size is increased supports the conclusion that $\mathscr{P}$ is the limiting scaling function. One generally expects the finite-size-scaling function to be analytic at $\tau_M=0$ as proven rigorously in Sec. IV for the short, fat $(\infty\times M)$ case. Although this has not been proved analytically in this general case, numerical calculations strongly favor this expectation.

VI. COMPARISON OF RESULTS FOR DIFFERENT LATTICE SHAPES

The analysis in the preceding section shows that the appropriate shape factor to hold constant as the thermodynamic limit is approached for the anisotropic K model is $\kappa=N^2/M$, where $2N$ is the number of lattice sites in the horizontal direction and $2M$ is the number of lattice sites in the vertical direction. We will now emphasize this point further by comparing the scaling functions $\mathscr{P}$ for the different cases studied in Secs. III–V. Recall that the finite-size-scaling functions are related to the specific heat per lattice site by Eqs. (3.13), (4.23), and (5.25) and that they apply in the limit as both the size of the system becomes infinite and the critical point is approached, (see Fig. 4.) The finite-size-scaling functions are functions of two variables. One variable is the shape factor κ. The other variable is a scaled temperature variable τ. In Sec. IV this scaled temperature variable was $\tau_M\sim Mt$ and in Sec. V this variable τ_M was used. However, in Sec. III this scaled temperature variable was $\tau_N\sim N^2t$ because τ_M is undefined for lattices of shape $N\times\infty$ where $M=\infty$. This inelegant difference in scaling variables can be eliminated by considering a new scaling variable τ defined by

$$\tau=\frac{\tau_M\tau_N}{\tau_M+\tau_N}=\frac{\kappa}{1+\kappa}\tau_M\sim\frac{MN^2}{M+N^2}t, \tag{6.1}$$

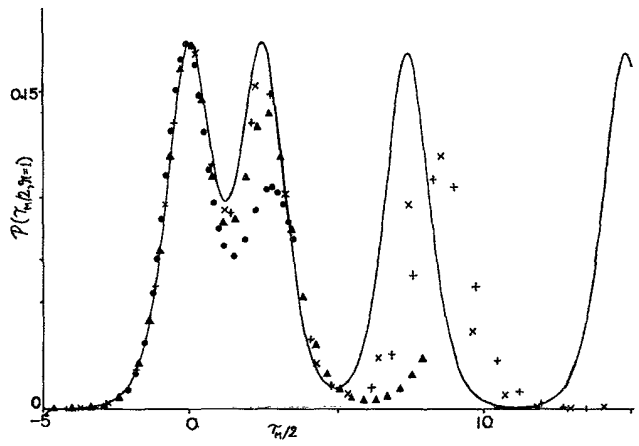

FIG. 7. Plot of the scaling function $\mathscr{P}(\kappa\tau_M/(1+\kappa),\kappa)$ versus $\tau_M/2$ for finite N and M with κ $(\equiv N^2/M)=1$. The functional form is given by Eq. (5.26). The numerically calculated points from Eq. (5.7) are: (i) ● for $N=4$, (ii) ▲ for $N=6$, (iii) + for $N=8$, and (iv) × for $N=10$. This multipeaked curve contrasts strongly with the single peaked curve in Fig. 5.

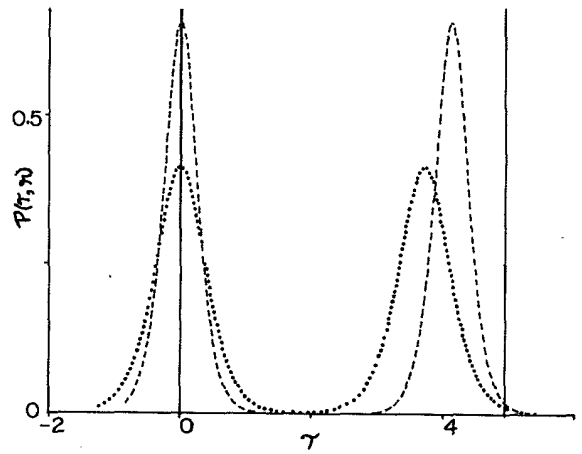

FIG. 8. Plots of $\mathscr{P}(\tau,\kappa)$ vs τ $[=\kappa\tau_M/(1+\kappa)]$ for different values of $\kappa<1$. (a) $\kappa=\frac{1}{3}$ (dotted curve), (b) $\kappa=\frac{1}{5}$ (dashed curve). The vertical lines indicate the δ-functions for $\kappa=0$ or equivalently the limiting scaling function $\mathscr{P}(\tau_N,0)$. (See Sec. III.) The position of the first peak remains fixed at $\tau=0$.

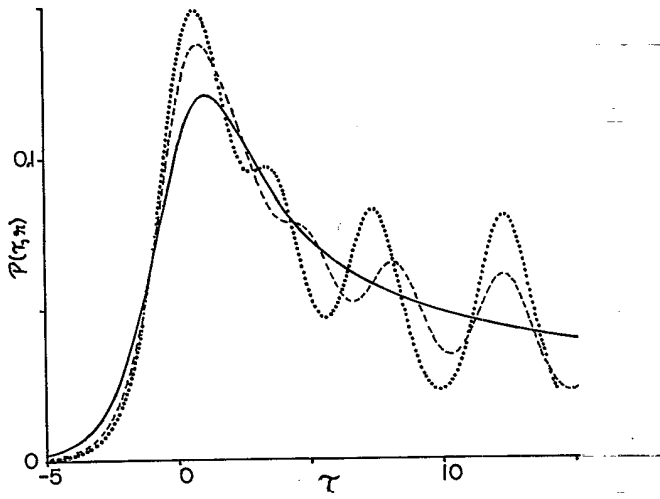

FIG. 9. Plots of $\mathcal{P}(\tau,\kappa)$ vs τ for different values of $\kappa>1$. (a) $\kappa=3$ (dotted curve), (b) $\kappa=5$ (dashed curve). The limiting form $\mathcal{P}(\tau_M,\infty)$, for shape $\infty\times M$, is shown by a solid line. The first peak for general κ approaches the single peak of $\mathcal{P}(\tau_M,\kappa)$ as κ tends to infinity.

where t is the reduced temperature.[3] For $\infty\times M$ shapes $\kappa=\infty$ and $\tau=\tau_M$. For $N\times\infty$ shapes $\kappa=0$ and $\tau=\tau_N$. For the same reason the generalized size variable $\mathcal{M}$, defined in Eq. (5.9), is used in Eq. (5.25). Note that $\mathcal{M}$ is equal to M for $\kappa=\infty$ but is equal to N^2 for $\kappa=0$. Therefore, the results for the scaling functions in Secs. III and IV are already expressed in terms of $\mathcal{P}(\tau,\kappa)$ in the limiting cases $\kappa=0$ and $\kappa=\infty$, respectively. For intermediate values of κ this variable τ is an appropriately generalized variable and this is the reason for using it, rather than τ_M, as an argument in Eq. (5.25).

Figure 8 shows $\mathcal{P}(\tau,\kappa)$ as a function of τ for three values of $\kappa<1$. The curves for $\kappa=\frac{1}{3}$ and $\frac{1}{5}$ were computed as described in Sec. V, Eq. (5.26) and the delta functions for $\kappa=0$ were computed in Sec. III, Eq. (3.13). Clearly, as κ is decreased toward 0, the scaling functions become more and more strongly peaked consistent with

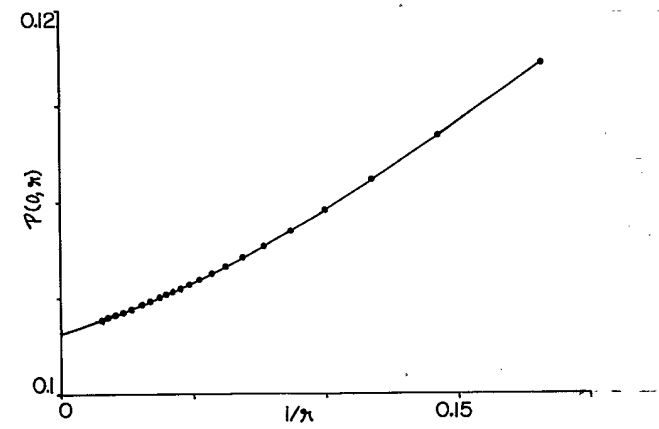

FIG. 10. Extrapolation plot of $\mathcal{P}(\tau=0,\kappa)$ vs $1/\kappa$. This extrapolation gives $\mathcal{P}(0,\infty)=0.103$ which agrees well with the corresponding value in Fig. 5.

approaching the limiting case of a sequence of delta functions when $\kappa=0$. The multiple peaks in the curve in Fig. 7 computed for $\kappa=1$ are then understandable as remnants of the δ functions for $r=0$. Figures 7 and 9 show what happens to the scaling functions as κ is increased. Figure 9 shows $\mathcal{P}$ for three values of $\kappa>1$. The functions for $\kappa=3$ and 5 were computed as described in Sec. V, Eq. (5.26) and the function for $\kappa=\infty$ was computed in Eq. (4.12) of Sec. IV and is also shown in Fig. 5. As κ increases from $\kappa=1$ the peaks become broadened and their amplitude decreases as seen in Fig. 9, until at $\kappa=\infty$ there is only one remaining peak which locates the pseudocritical temperature [see Eq. (4.24)] for the $\infty\times M$ geometry.

Figures 7–9 show that there is an orderly progression of the scaling function, $\mathcal{P}(\tau,\kappa)$ as a function of both variables, τ and κ. This orderly dependence upon κ is also indicated in Fig. 10, where the scaling function is shown as a function of $1/\kappa$ at one temperature, namely the critical temperature, $\tau=0$. The limiting value as $1/\kappa$ approaches zero is in good agreement with the value, $\mathcal{P}(0,\kappa=\infty)=0.103$, computed in Sec. IV, Eq. (4.12) and also calculated numerically in Fig. 6. Such consistency provides another check on the more difficult calculations performed in Sec. V.

VII. CONCLUSIONS

The central conclusion in this paper is that finite-size-scaling theory works asymptotically close to the critical point of the K model. This conclusion would be of no surprise for the usual sort of magnetic or fluid models. However, it was not a foregone conclusion for the K model because of its unusual forcing constraint, its long-range correlation functions at all temperatures above T_c, and its highly asymmetric specific-heat divergence at T_c.

The finite-size-scaling functions, $\mathcal{P}(\tau,\kappa)$, obtained in this paper (see Figs. 5 and 7–10) reflect the anisotropic nature of the K model. This can be made clear by comparing with a well-known system, namely, the two-dimensional Ising model. One can define an anisotropic square lattice Ising model by using two different coupling constants in the two principal directions. However, close to the critical point isotropy develops asymptotically so that even the finite-size effect for the anisotropic model is qualitatively similar to the isotropic model. In other words the anisotropy is not relevant for the critical behavior. The relevant shape factor for such an anisotropic model will be the ratio $\delta=N/M$ as one would guess for an isotropic model. The scaling function $\mathcal{P}$ in Eq. (1) for $\delta=0$ and $\delta=\infty$ will be the same if appropriate variables are used. In contrast, for long, thin $N\times\infty$ shapes ($\kappa=0$) of the K model $\mathcal{P}(\tau,\kappa)$ is a series of δ functions in τ and for $\kappa=\infty$ (short, wide $\infty\times M$ shapes) $\mathcal{P}(\tau,\kappa)$ is a smooth typical finite-size-scaling function. This difference shows the relevance of the anisotropy of the K model. We have shown that, despite these differences, $\mathcal{P}$ interpolates smoothly as a function of κ between the two extremes, and so there is no question that there is one unified scaling function of both variables τ and κ.

The scaling variables for the K model contain impor-

tant information. Asymptotically, they are given by

$$\tau \sim MN^2 t/(M+N^2) \tag{7.1}$$

and

$$\kappa = N^2/M \ . \tag{7.2}$$

These scaling variables also exhibit the anisotropy of the K model because the linear dimensions along the two mutually perpendicular directions do not enter with the same powers. For $\kappa=0$ one has $\tau \sim N^2 t$; by the central dogma of finite-size-scaling theory this implies that there exists a length scale ξ_x along the horizontal (or N) direction diverging as $t^{-1/2}$ for the bulk or $\infty \times \infty$ lattices. For $\kappa=\infty$ one has $\tau \sim Mt$; according to finite-size-scaling theory this implies the existence of another length scale ξ_y along the vertical (or M) direction diverging as t^{-1} for the bulk or $\infty \times \infty$ lattices. To obtain a finite-size-scaling function of the single variable τ different from $\mathcal{P}(\tau,0)$ or $\mathcal{P}(\tau,\infty)$ requires holding κ fixed, meaning that the vertical M dimension of the lattice grows proportionally to the square of the horizontal N dimension. This is exactly what one would expect if the length scale in the vertical direction diverges as t^{-1} which is the square of the asymptotic divergence $t^{-1/2}$ in the horizontal direction. Therefore, these finite-size-scaling variables provide very strong evidence that the critical exponents for the divergence of the length scales of the bulk system near the critical point are indeed anisotropic with $\xi_x \sim t^{-1/2}$ ($\nu_x=\frac{1}{2}$) and $\xi_y \sim t^{-1}$ ($\nu_y=1$). These values of ν_x and ν_y are in agreement with the general phenomenological theory.[21,20] However, these values of ν_x and ν_y deduced from finite-size-scaling theory should also be substantiated with direct calculations of the correlation functions for the bulk system. Therefore, at present we prefer to describe the inverse powers of N and M that appear in the scaling variables as ν_N and ν_M. We conclude that we have calculated the values $\nu_N=\frac{1}{2}$ and $\nu_M=1$ exactly and that it is very likely that $\nu_N=\nu_x$ and $\nu_M=\nu_y$.

ACKNOWLEDGMENTS

We thank David A. Huse for pointing out a mathematical identity that led to a helpful simplification. This paper is based in part on a portion of the Ph. D. thesis of S. M. B. at Carnegie Mellon University. This research was supported by National Science Foundation Grant No. DMR-81-15979.

APPENDIX A: PARTITION FUNCTION FOR SECTION IV

Using the whole range of ϕ_1 [Eqs. (2.5) and (2.6)], one can rewrite Eqs. (2.9) and (2.10) as

$$\ln(\Upsilon_j Z_j) = \begin{cases} \sum_{n=1}^{N} \ln\left[(-1)^{-j} + (s(n\pi/N))^{2M}\right] & (\text{for } j=1,2) \quad \text{(A1)} \\ \sum_{n=1}^{N} \ln\left[(-1)^{-j} + [s((n-\frac{1}{2})\pi/N)]^{2M}\right] & (\text{for } j=3,4)\ . \quad \text{(A2)} \end{cases}$$

In the limit $N \to \infty$ these sums can be replaced by the following integrals:

$$\mathcal{I}_j = \frac{N}{\pi} \int_0^{\pi} \ln[(-1)^{-j} + s^{2M}(\phi)]d\phi \tag{A3}$$

so that

$$Z_j = \Upsilon_j \exp(\mathcal{I}_j) \tag{A4}$$

with $\mathcal{I}_1=\mathcal{I}_3$ and $\mathcal{I}_2=\mathcal{I}_4$. From Eqs. (A4), (2.3), and (2.1) and exploiting the symmetry of $\cos\phi$ about $\phi=0$ one obtains Eq. (4.1).

APPENDIX B: EVALUATION OF J_r

Equation (4.7) can be written as

$$\exp(-\tau r)J_r = \int_0^q \exp(-Mr\phi^2)d\phi + R_1 + R_2\ , \tag{B1}$$

where

$$R_1 = \int_q^{\pi/2} \exp(2Mr \ln\cos\phi)d\phi\ , \tag{B2}$$

$$R_2 = \int_0^q (\exp(-Mr\phi^2))[\exp(2Mr\ln\cos\phi + Mr\phi^2) - 1]d\phi\ . \tag{B3}$$

and q [$\sim O(1)$] is an undetermined number close to zero. The first significant term of the Taylor expansion of $\ln\cos\phi$ is used to obtain the first term on the rhs of Eq. (B1). From Eq. (B2) we have

$$|R_1| < b\exp(2Mr\ln\cos q)\ , \tag{B4}$$

for some constant b so that R_1 is exponentially small for $q \sim O(1)$. Therefore when summed over r, its contribution to I in Eq. (4.6) is also exponentially small. For R_2, we note that $\exp(2Mr\ln\cos\phi + Mr\phi^2) - 1$ is analytic in the neighborhood of $\phi=0$ and therefore can be expressed in a uniformly convergent series in that region. We write it as

$$1 - \exp(2Mr\ln\cos\phi + Mr\phi^2) = 1 - \exp\left[\sum_{k=2}^{\infty} a_k (Mr\phi^2)^k/(Mr)^{k-1}\right]\ , \tag{B5}$$

where a_k's are the coefficients of the expansion of the argument of the exponential. It therefore follows that the leading term of Eq. (B5) gives the leading M dependence of R_2 and its magnitude is

$$|a_k| Mr \int_0^q \phi^4 \exp(-Mr\phi^2)d\phi < Br^{-3/2}M^{-3/2} \tag{B6}$$

for some constant B. The last inequality is obtained by extending the range of integration to infinity. Extending the range of integration of the first term of Eq. (B1) to infinity introduces an error

$$R_3=\int_q^\infty \exp(-Mr\phi^2)d\phi \tag{B7}$$

which, being in the form of the error function, is exponentially small as $M\to\infty$. Hence the significant error is from Eq. (B6) which when inserted into Eqs. (4.6) and (4.2) yields an error of order $O(M^{-1/2})$ to the specific heat while the leading term is $O(M^{1/2})$.

APPENDIX C: EVALUATION OF S_l

We write S_l in Eq. (5.12) as

$$\exp(-l\tau_M)S_l=S_{1l}+S_{2l}\ , \tag{C1}$$

where

$$S_{1l}=\sum_{n=1}^{q}\exp\left[2\kappa M\ln\cos\left[\frac{n\pi}{N}\right]\right], \tag{C2}$$

$$S_{2l}=\sum_{n=q+1}^{p}\exp\left[2\kappa M\ln\cos\left[\frac{n\pi}{N}\right]\right], \tag{C3}$$

and $q<N/2$ is to be determined later. For S_{2l} we have

$$S_{2l}<(\tfrac{1}{2}N-q-1)\exp[2lM\ln\cos(q\pi/N)]\ . \tag{C4}$$

and we write S_{1l} as

$$S_{1l}=\sum_{n=0}^{\infty}\exp(-l\pi^2n^2/\kappa)+\mathscr{R}_1+\mathscr{R}_2\ , \tag{C5}$$

where

$$\mathscr{R}_1=\sum_{0}^{q}[\exp(-l\pi^2n^2/\kappa)]\times\{\exp[2lM\ln\cos(n\pi/N)+l(\pi n)^2/\kappa]-1\}\ , \tag{C6}$$

and

$$\mathscr{R}_2=\sum_{q+1}^{\infty}\exp(-l\pi^2n^2/\kappa)\ . \tag{C7}$$

The leading M dependence of $\mathscr{R}_1$ can be estimated along the same line as done in Appendix B for R_2. The leading term for $\mathscr{R}_1$ is now

$$|a_2|lN^{-2}\sum_{n=0}^{q}n^4\exp(-l\pi^2n^2/\kappa)<\delta l^3N^{-2}q\ , \tag{C8}$$

where δ is some constants. The last inequality is obtained by replacing $x^n\exp(-ax)$ by its maximum term at $x=n/a$. When all the above contributions to S_{1l} and S_{2l} are combined and summed over l to obtain $\ln Z_2$ in Eq. (5.11), we choose $q\sim N^\eta$ with $0<\eta<1$ so that $\mathscr{R}_2$ is $O(N^{-2+\eta})$. For this choice of q both S_{2l} and $\mathscr{R}_1$, the latter of which can be estimated via error functions as in Appendix B, are exponentially small.

*Present address: Department of Polymer Science and Engineering, University of Massachusetts, Amherst, MA 01003.

[1]P. W. Kasteleyn, J. Math. Phys. **4**, 287 (1963).
[2]J. F. Nagle, Phys. Rev. Lett. **34**, 1150 (1975).
[3]We are using the conventional notations, namely, $\beta=(k_BT)^{-1}$, where T is the temperature and k_B is the Boltzmann constant. The specific-heat exponent α is given by $c(t)\sim t^{-\alpha}$ as $t\to0$, where c is the specific heat and t is the reduced temperature $(T-T_c)/T_c$. For the length scale ξ_i the exponent ν_i is given by $\xi_i\sim t^{-\nu_i}$ for $i=x,y$ as $t\to0$. For an isotropic system the subscript i may be omitted.
[4]P. W. Kasteleyn, Physica (Utrecht) **27**, 1209 (1961).
[5]H. N. Temperley and M. E. Fisher, Philos. Mag. **6**, 1061 (1961).
[6]B. M. McCoy and T. T. Wu, *The Two Dimensional Ising Model*, (Harvard University, Cambridge, Mass., 1973).
[7]L. Onsager, Phys. Rev. **65**, 117 (1944).
[8]M. E. Fisher, J. Math. Phys. **7**, 1776 (1966).
[9]S. R. Salinas and J. F. Nagle, Phys. Rev. **B9**, 4920 (1974).
[10]J. F. Nagle and G. R. Allen, J. Chem. Phys. **55**, 2708 (1971).
[11]J. F. Nagle, J. Chem. Phys. **58**, 252 (1973).
[12]M. E. Fisher, Phys. Rev. **124**, 1664 (1961).
[13]B. Sutherland, Phys. Lett. **26A**, 532 (1968).
[14]C. S. O. Yokoi and S. Salinas (unpublished).
[15]J. F. Nagle, Ann. Rev. Phys. Chem. **31**, 157 (1980).
[16]P. Bak, Rep. Prog. Phys. **45**, 587 (1982).
[17]S. M. Bhattacharjee, J. F. Nagle, D. A. Huse, and M. E. Fisher, J. Stat. Phys. **32**, 361 (1983).
[18]M. E. Fisher, J. Stat. Phys. **34**, 667 (1984).
[19]S. M. Bhattacharjee, Phys. Rev. Letts. **53**, 1161 (1984).
[20]D. A. Huse and M. E. Fisher, Phys. Rev. B **29**, 239 (1984).
[21]H. J. Schultz, Phys. Rev. B **22**, 5274 (1980).
[22]M. N. Barber, in *Phase Transitions and Critical Phenomena*, edited by C. Domb and J. Lebowitz (Academic, London, 1983), Vol. 7, p. 146.
[23]N. G. de Bruijn, *Asymptotic Methods in Analysis*, 3rd ed. (Dover, New York, 1981), Chap. 3.
[24]A. E. Ferdinand, J. Math. Phys. **8**, 2332 (1967).
[25]A. E. Ferdinand and M. E. Fisher, Phys. Rev. **185**, 832 (1969).
[26]S. M. Bhattacharjee, Ph.D thesis, Carnegie Mellon University, 1984.
[27]In Ref. 7 the partition function is written as $Z=(-Z_1+Z_2+Z_3+Z_4)/2$. However we have incorporated the minus sign associated with Z_1 in the definition in Eq. (2.2).
[28]V. L. Pokrovksy and A. L. Talapov, Phys. Rev. Lett. **42**, 65 (1979).
[29]T. Izuyama and Y. Akutsu, J. Phys. Soc. Jpn **51**, 50 (1982).
[30]International Mathematical and Statistical Libraries subroutines, available from IMSL, Inc., Houston, Texas 77036-5085.